New Approach for Representation of Molecular Surface

WENSHENG CAI,[1,2] MAOSEN ZHANG,[1] BERNARD MAIGRET[2]

[1]*Department of Applied Chemistry, University of Science and Technology of China, Hefei, Anhui, China*

[2]*Laboratoire de Chimie Theorique, Université Henri Poincaré Nancy I BP 239, 54506 Vandoeuvre-lès-Nancy, France*

Received 8 May 1998; accepted 16 June 1998

ABSTRACT: A new algorithm is proposed for approximation to the molecular surface. It starts with a triangular mesh built on an ellipsoid embracing the whole molecular surface. The triangular mesh is obtained from an icosahedron subdivision sphere with highly uniform vertex distribution, and the embracing surface is deflated stepwise to the best adherence of its triangles onto the surface of the molecule. The deflating direction of each vertex of a triangle is defined by the vector normal at this point to the previous deflated embracing surface. Our results show that the speed of the triangulation embracing ellipsoid method and the quality of the surface obtained by the method are faster and better than the method that starts with a quadrilateral mesh built from meridian and parallel representations on an embracing sphere to get the molecular surface. Furthermore, the surface obtained by the method can be used directly to approximate the molecular surface by spherical harmonic expansions.
 J Comput Chem 19: 1805–1815, 1998

Keywords: molecular surface; molecular graphics; molecular recognition

Introduction

Calculation, representation, and manipulation of molecular surfaces are important, not only for understanding molecular stability and recognition, but also for prediction of three-dimensional (3D) structures of biological macromolecules and assemblies:

- The area of the accessible surface has been shown to be related to hydrophobic free energies of solvation,[1,2] and the free energy and enthalpy of solvation have recently been approximated in protein calculations by a simple relation involving surface calculations.[3–11]

Correspondence to: B. Maigret

Contract/grant sponsors: Centre National de la Recherche Scientifique; Academy Sinica; CNRS–K. C. Wong Postdoctoral Fellowship

CCC 0192-8651 / 98 / 161805-11

- Given the binding site of a protein, the possible ligands presenting lock-and-key surface complementarity[12] can be identified. Studies of complementarity between ligands and their receptors have shown that loss of solvent-accessible surface area, and/or complementarity in shape and charge distributions, are the major determinants of affinity and specificity.[13–18] Similarly, complementarity of hydrophobicity now seems well established for the packing of helices in proteins.[13,14] Several attempts have recently been proposed using different techniques[19–27] for studying the shape complementarity between proteins, and between proteins and their ligands.
- Electrostatic and shape complementarity at protein–protein interfaces are recognized as key features for protein recognition, and computing the electrostatic field around a macromolecule using the boundary element method (BEM) implies that the molecular surface is properly evaluated.[28–31]
- In protein engineering and prediction, the knowledge of how the constituting pieces of secondary structure or folding domains can pack together is of crucial importance for the establishment of a reliable model of native conformation.[32,33]

In these studies, the protein–protein and protein–ligand interactions are crucially important. But detailed analysis of molecular interactions is computationally expensive. Approximation of the molecular surface has been used to assess the interactions between molecular surfaces, such as simplified representation based on expansions of spherical harmonic functions.[34,35] The spherical harmonic surface is useful for studying the motion of macromolecules and the interaction between them. But, it is first necessary to map the original surface to a unit sphere. Duncan and Olson described this topological mapping procedure in creating the spherical harmonic approximation to the molecular surface.[35] The topological mapping program smoothly transforms the molecular surface computed by Connolly's program[36,37] onto a unit sphere, and spherical harmonic coefficients are computed. We present here another method for performing the topological mapping step by mapping an ellipsoid to the molecular surface. The embracing molecular surfaces obtained are topologically equivalent to a sphere, and each point on the molecular surface has a unique spherical coordinate (θ, φ) on a unit sphere. Therefore, the spherical harmonic expansion coefficients can be computed directly from the Cartesian coordinates and their spherical coordinates.

Method

The concepts of solvent-accessible surface and molecular surface were brought forth by Lee and Richards[38] and Richards.[39] The solvent-accessible surface of Lee and Richards was defined as the locus of the center of an imaginary spherical probe of given radius (usually 1.5 Å) representing a solvent molecule as it rolls along the outside of the molecule while maintaining contact with the van der Waals surface (Fig. 1). The improvement definition is the molecular surface represented by Richards (Fig. 1), which is the combination of the part of the van der Waals surface accessible to the probe sphere (the contact surface) and of the part of the probe sphere looking toward the molecule when it is in contact with more than one atom (the re-entrant surface). Based on the definition, the molecular surface consists of convex pieces, toroidal pieces, and concave pieces. Because this definition can lead to self-intersecting surfaces, Connolly proposed methods[36,37] to calculate the molecular surface with the intersecting regions trimmed away. This surface is referred to as "solvent-excluded," which Sanner and Olson[40] defined as the topological boundary of the union of all possible probes having no intersection with the molecule.

In the present study, the molecular surface is the solvent-excluded surface. It is determined by the coordinates of atoms in the target molecule, their van der Waals radii, and the probe radius. Depending on the radius of the probe, rp, we can obtain the van der Waals surfaces ($rp = 0.0$ Å) or the molecular surfaces ($rp > 0.0$ Å). The surface resulting from this method is a triangular mesh that closely adheres to a molecular surface. This triangular mesh is not created by subdividing the curved faces of an analytical molecular surface, but rather is obtained by mapping a triangular mesh distributed on an ellipsoid to a molecular surface. The starting ellipsoid embraces all atoms in the molecule. The mapping procedures from the ellipsoid to the molecular surface are achieved by deflating the triangular meshes stepwise. For this

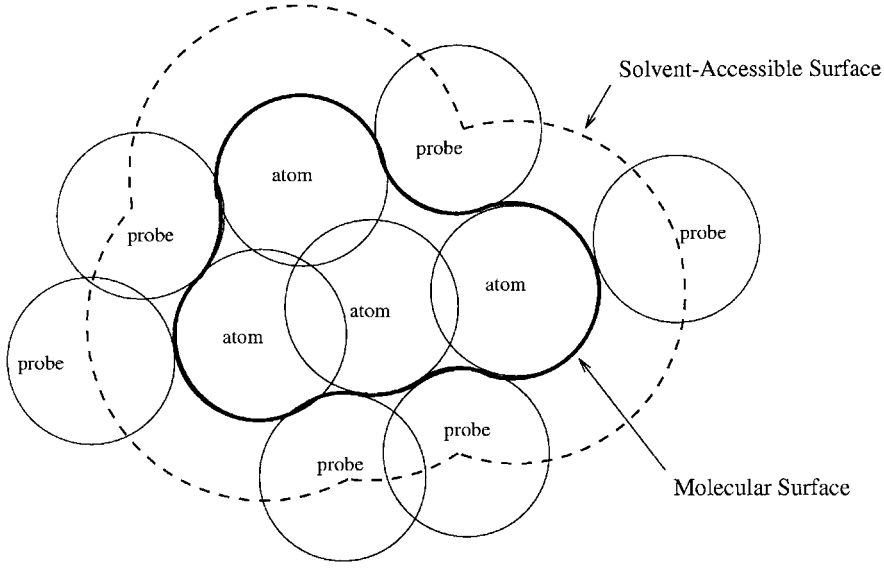

FIGURE 1. Definition of solvent-accessible surface and the molecular surface.

purpose, the following stepwise scheme is applied:

1. Building of a starting ellipsoid embracing the whole molecular surface, and of the associated triangular mesh starting from an icosahedron subdivision sphere.
2. Analytical determination of all pieces of the molecular surface.
3. Stepwise deflation of the ellipsoid so that all vertices of the triangles on the embracing surface arrive on the molecular surface.

DEFINITION OF STARTING ELLIPSOID EMBRACING ENTIRE MOLECULAR SURFACE

In our method, the starting embracing ellipsoid is not the envelope of minimum radius that includes all van der Waals atomic spheres. To avoid unexpected problems during stepwise deflation (it is necessary that the embracing surface always surrounds the molecular surface during the deflation, and that the moving grid never runs through itself), the following procedures were used:

1. Calculate the center of mass of the molecule. If it is located inside the van der Waals sphere of an atom, then this atom is taken as the center of the starting embracing ellipsoid; otherwise, the closest atom is chosen for the purpose.
2. Compute the principal axes and direction cosines of principal vectors relative to the working Cartesian system.

The direction cosines and the semiaxis lengths for three principal axes of the ellipsoid (Fig. 2) are calculated as follows:

(i) Let atom i be the furthest atom from the center of the ellipsoid O, thus the greatest axis OX' should be the unit-length vector from the center O to atom i and its semiaxis length a should be $a = d_i + r_i$, where d_i is the distance from the center of ellipsoid O to atom i, and the r_i is the van der Waals radius of atom i.

(ii) Translate and rotate the molecule to make the center O at the origin and the greatest axis at the direction of the X-axis.

(iii) Calculate the middle axis OY', and its semiaxis length b. For each atom, n, on the plane that consists of OX' and the center of the atom, find an ellipsoid embracing the atom and tangent to it. Then the semiaxis length of middle axis b_n can be determined. Take the greatest one b_j in b_n ($n = 1$, number of atoms) as b, the corresponding plane as the main plane that contains the greatest axis OX' and middle axis OY', on which the ellipsoid will include, and tangent to the sphere of atom j which makes this ellipsoid to be of the greatest semiaxis length of the middle axis among all atoms (Fig. 2a).

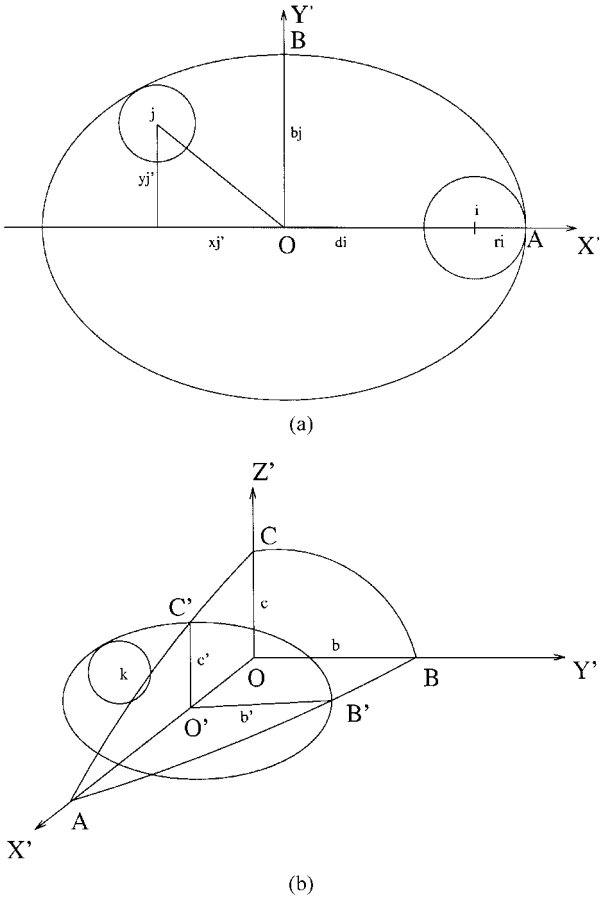

FIGURE 2. Calculation of three principal axes and their semiaxis lengths of the embracing ellipsoid. (a) Atom *i* is the furthest one from the ellipsoid center *O*, $a = d_i + r_i$. Atom *j* has the greatest b_j, with semiaxis length *a* and *bj* the ellipsoid (*OAB*) will include and tangent to it, $b = b_j$. (b) Atom *k*, on which the corresponding intersection ellipsoid *O′B′C′*, orthogonal to the ellipsoid *OAB*, containing and tangent to the atom, makes the embracing ellipsoid of the greatest semiaxis length *c*.

(iv) Calculate the shortest axis OZ' and its semiaxis length c. The shortest axis of ellipsoid OZ' should be $OX' \times OY'$, and its semiaxis length, c, can be calculated in a manner similar to before. In Figure 2b, b' and c' are the semilengths of the principal axes of the ellipsoid $O'B'C'$. Ellipsoid $O'B'C'$ is orthogonal to the $OX'Y'$ plane and tangent to atom k, which makes the semiaxis length of the shortest axis c the largest one. By the same method we calculate c'. Then, c can be obtained from the ellipsoid equation.

We now have the ellipsoid with three principal axes, OX', OY', OZ', and their semiaxis length a, b, c, which includes the whole molecular surface. We first approximate an ellipsoid whose semiaxis lengths are the unit lengths to obtain the equilateral triangular mesh of this ellipsoid (sphere) from an icosahedron subdivision sphere. This procedure involves subdividing triangles by connecting midpoints and was already used for molecular display[41] for providing the advantage of a highly uniform vertex distribution. The numbers of vertices and triangles in the final sphere surface are $12 + 10 \times (4^n - 1)$ and 20×4^n, respectively, where n is the recursion depth or subdivision number. We then change the orientation and scale according to the direction cosines of the three principal axes and the three semiaxis lengths just calculated. Thus, we may obtain each grid point of all the triangles on the embracing ellipsoid surface. As an example, the starting triangulation ellipsoid for a molecule with 642 points and 1280 triangles is shown on Figure 3.

DETERMINATION OF PIECES OF MOLECULAR SURFACE

Our molecular surface can be described by three types of surface pieces (Fig. 4):

1. Convex spherical pieces obtained directly from the van der Waals spheres of the atoms, when the imaginary probe is in contact with one atom.

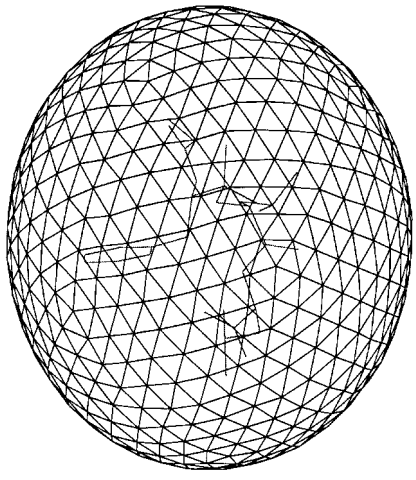

FIGURE 3. The icosahedron-derived embracing ellipsoid. The triangular mesh has 642 vertices and 1280 triangles. The molecule embraced is thermolysin substrate (PDB code 7tmn, 33 atoms).

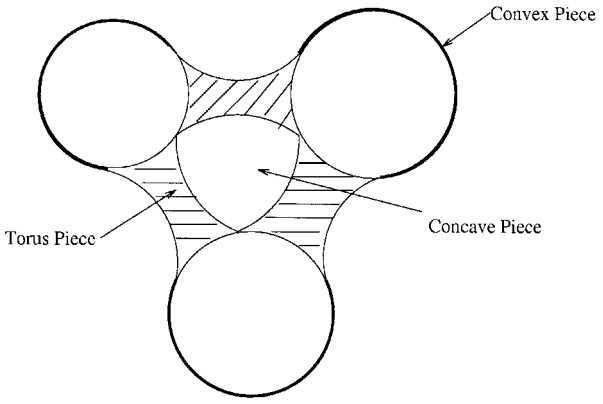

FIGURE 4. Three types of surface pieces: the convex pieces (part of the van der Waals spheres of the atoms); the concave pieces (spherical triangles on the probe sphere facing the molecule, when it contacts with three atoms); and the tori pieces (defined by the probe when it rolls over two atoms).

2. Concave spherical pieces (spherical triangles) arising from three neighboring atoms, when the imaginary rolling sphere is simultaneously tangent to each of them, the inward-facing part of the probe sphere.
3. Toroidal pieces related to two atoms, when the imaginary probe sphere is simultaneously tangent to their van der Waals spheres and rolled around them, formed by the inward-facing arc on the probe connecting the two tangent points.

To calculate the molecular surface from these constitutive elementary pieces, it is first necessary to see how each piece is contiguous with respect to another, so that the resulting embracing surface will be continuous. For that purpose, the following definitions are introduced:

1. A convex piece of sphere and a torus is considered contiguous if the atom from which the convex piece comes is one of the two atoms from which the torus is obtained.
2. Similarly, a convex piece of sphere and a concave piece will be considered contiguous if the atom generating the convex part belongs to the triplet of atoms defining the concave piece.
3. A concave piece of sphere and a torus will be contiguous if the two atoms defining the torus belong to the triplet defining the concave piece.

Now, given the spatial positions of all atoms in a molecule and their associated van der Waals radii, and a radius value for the rolling imaginary sphere, it is possible to calculate analytically the variously shaped pieces contributing to the molecular surface.[36] Each convex piece is defined by an atomic van der Waals sphere, which is defined by the atomic center and the atomic radius. Each concave piece is defined by a spherical triangle, which is defined by a probe position, the probe radius, and three tangent points. Each torus is defined by a center of the circle traced by the probe center, two radii, and an axial vector through the atom centers.

ITERATIVE DEFLATION OF STARTING EMBRACING ELLIPSOID

The deflation of the starting envelope ellipsoid, giving an embracing surface as close as possible to the molecular surface, is performed iteratively for each triangle vertex in a direction defined by the vector normal at this point to the previous deflated embracing surface. The iterative deflation procedure is:

1. For each triangle vertex, P, calculate its next position, P', along its deflating direction with a given step size.
2. If segment PP' intersects any local embracing sphere of any surface piece, go to step 3, otherwise, set P to P' and go to step 1.
3. If segment PP' does not intersect any surface piece (convex, torus, or spherical triangle), set P to P' and go to step 1. Otherwise, calculate the first intersecting point between PP' and the surface pieces that intersect it.
4. Repeat this procedure until all triangle vertices arrive the molecular surface.

Direction of deflation. Given a deflation step i, we define a triangle adjacent to a vertex P by P itself and by two vertices adjacent to P. The vector interiorly normal to the embracing surface at P is evaluated by the average vector obtained from all vectors normal to all adjacent triangles (Fig. 5). This average vector will give the usual deflating direction of the $i + 1$ deflation at point P. Thus, the next position of point P (P') can be calculated by its deflating direction and the step size. The iterative step size will influence the final position of each point and the stability of the algorithm. In our study, the value of the step size is a constant

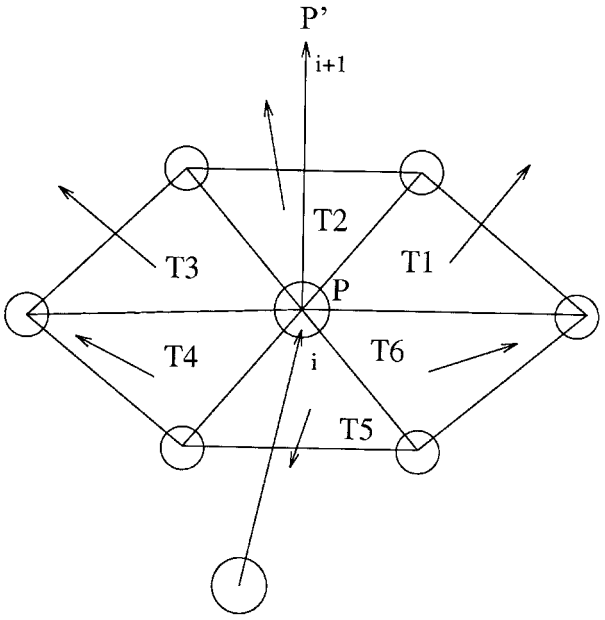

FIGURE 5. The deflating direction of point *P* is the average vector of the interior normal vector of its adjacent triangles (T1, T2, T3, T4, T5, T6). *P'* is the next position of point *P* along this direction.

(usually 1.4 Å). As soon as a vertex reaches the molecular surface, it is kept fixed at this position during the following steps. These fixed vertices will drive the envelope surface in the iterative procedure toward the molecular surface as close as possible.

Local embracing sphere. During this iterative procedure, all possible intersections between each molecular surface element (piece of sphere, spherical triangle, and torus) and each segment on the deflating direction of each point on the deflating surface should be calculated.

As most of the deflation steps will not intersect the molecular surface, a test procedure has been introduced to save computer time. This procedure calculates the ''distance'' between a point and a molecular surface element using a local embracing sphere associated with each molecular surface element as follows:

1. For a convex piece of sphere, the local embracing sphere will be the van der Waals sphere of the associated atom.
2. For a spherical triangle, the center of the local embracing sphere will be the orthogonal projection of the center of the imaginary rolling sphere on the plane defined by the center of the three atoms from which this molecular surface element is obtained (Fig. 6a). The radius of this local embracing sphere will be the maximum distance between its center and the vertex of the spherical triangles.
3. In the case of tori, the local embracing sphere center will be the center of the circle defined by the centers of all the rolling imaginary spheres tangent to the two atoms defining the torus (Fig. 6b). The radius of the local embracing sphere will be the maximum distance between its center and the two tangent points defining the torus.

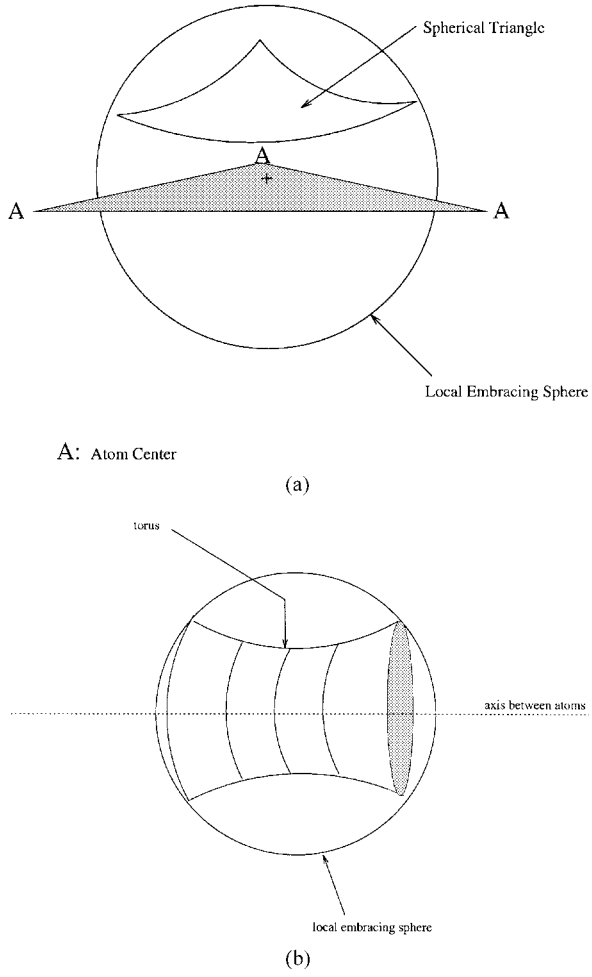

FIGURE 6. (a) Definition of a local embracing sphere around a spherical triangle. (b) Definition of a local embracing sphere around a torus.

Intersection. Let us consider any grid point *P* at any step *i* of the deflation, and any other point *Q* on its deflation vector (Fig. 7). First, the segment *PQ* cannot intersect the molecular surface pieces if their local embracing spheres do not intersect. After the segment *PQ* intersects the local embracing

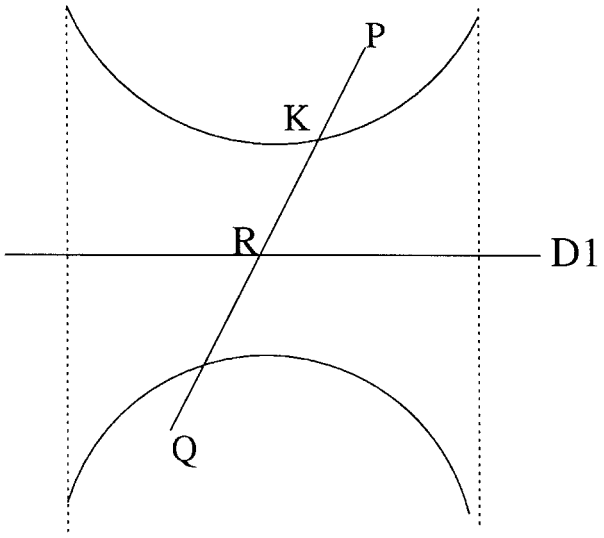

FIGURE 7. Intersection on the plane containing the segment *PQ* and parallel to *D*, the symmetry axis of the torus. *D*1 is the projection of *D* in this plane. To calculate the first intersection point *K* (nearest to *P*) on the segment *PQ*, it is necessary to verify if: (1) *Q* is inside the embraced volume or not; (2) *R* is a point on the segment *PQ* or not; and (3) *R* is inside the embraced volume or not.

spheres, the first intersection, *K* (nearest to *P*), between segment *PQ* and the molecular surface, can be computed. Intersections with spheres and spherical triangles can be easily computed, and only tori require attention. For instance, let *D* be the symmetry axis of the torus. Intersection can be easily seen on the plane containing the segment *PQ*, parallel to *D*. The projection, *D*1, of *D* in this plane is also a symmetry axis for this view. Let *R* be the intersection between *D*1 and the segment *PQ*; we can see in Figure 7 that it is necessary to verify the following events:

1. *Q* is inside the volume embraced by the torus, or not.
2. *R* is a point on the segment *PQ*, or not.
3. *R* is inside the volume embraced by the torus, or not.

If *Q* is inside the volume, calculate the intersection of *PQ* with the torus. Otherwise, only when *R* is a point on segment *PQ* and *R* is inside the volume, can the intersection of *PQ* with the torus be calculated by the method.

It should be noted that, because the self-intersecting pieces should be trimmed away, intersections in this region cannot be considered points on the molecular surface. During the deflation procedure, the first intersection of a vertex is considered as its final position on the molecular surface.

After all triangle vertices arrive the molecular surface (i.e., all possible intersections have been computed) the iterative procedure will stop. A triangulated molecular surface mapped from the triangular mesh on the ellipsoid is obtained.

Implementation of the algorithm. Two independent parts are included in our programs. One is written in FORTRAN-77 to create all vertices of triangles on the molecular surface and their connectivity. The other part is written in C^{++} to display the smooth surface using the previous results. These have been implemented for SGI Graphics workstations.

The approach presented here requires four successive steps:

1. The first procedure calculates the starting embracing ellipsoid and builds the uniform triangular mesh on it by subdivision of an icosahedron on a sphere. The number of triangles on the surface can be chosen depending on the size of the molecule.
2. The second procedure performs an analysis of the elements of the molecular surface from its atomic coordinates.
3. The third procedure concerns the deflation and convergence toward the best embracing surface starting from the ellipsoidal surface. Figure 8 shows two successive deflating steps for an example molecule of 26 atoms.
4. The final procedure concerns the graphical display of the smooth embracing surface on raster graphics terminals. We used polygonal Gouraud shading to display such pictures.

Results and Discussion

CPU TIMES FOR ELLIPSOID, SURFACE PIECES, AND DEFLATION CALCULATIONS

Table I shows the CPU times (on an SGI Iris Indy) required to calculate the embracing ellipsoid with a triangular mesh, and to determine analytically all the pieces (convex, toroidal, and concave faces) of molecular surfaces for several molecules; the radius of probe *rp* is 1.5 Å. The CPU time is related to the number of atoms and the number of triangles on the mesh. The latter CPU time depends mainly on the number of triplets of atoms possibly producing a concave spherical piece of

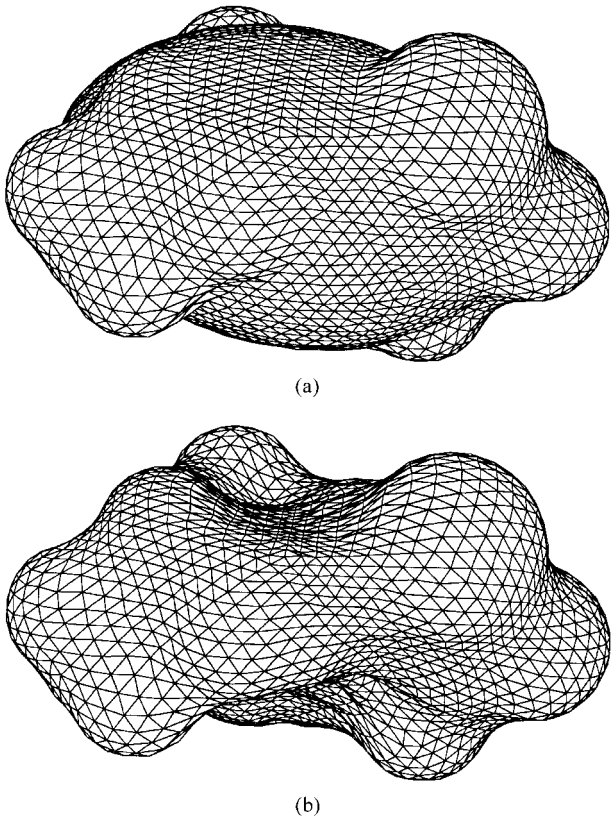

FIGURE 8. Triangular mesh surface with hidden-line removal of two successive deflating steps for a small molecule with 26 atoms. (a) The embracing surface at step 4 (radius of probe = 1.5 Å, number of vertices = 2562, number of triangles = 5120, step size = 0.5 Å, step = 4). (b) The final molecular surface (radius of probe = 1.5 Å, number of vertices = 2562, number of triangles = 5120, step size = 0.5 Å, step = 7).

molecular surface (some triplets of atoms cannot contact with the probe), which is determined by the atomic coordinates, radii, and the radius of the probe sphere.

Table II gives the deflating steps used and the CPU times (on an Iris Indy) required when deflating the starting ellipsoid surface to the solvent-accessible surface (just increasing the radius of each atom by the radius of the probe 1.5 Å, then setting the radius of the probe to 0.0 Å) for five molecules, when the deflation step size equals 10.0 Å and 1.4 Å. Table III gives the CPU times for the corresponding molecular surfaces (the radius of the probe is 1.5 Å), when the deflation step size equals 1.4 Å. The average CPU times of each step for each molecule are also listed in Tables II and III. During each step of the deflation process it is necessary to calculate the intersections of the triangles with the molecular surface pieces, and the number of such intersections depends on the number of moving grid points (the vertices of the triangles) at this deflation step and the number of the surface elements. From Table II, we can see that, besides the number of surface pieces and the number of triangles, the deflation step size also affects the deflation time. The smaller step size will increase the deflation time, but it can be beneficial in increasing the stability of the algorithm. The calculation results for the molecular surfaces of these molecules when the step size is 10.0 Å are not convergent.

The total CPU time to generate the solvent-accessible surface or molecular surface from atomic coordinates of the molecule can be calculated from Tables I and II, or Table III. For example, for the thermolysin substrate molecule with 33 atoms (the PDB code is 7tmn), the CPU time to generate the molecular surface (number of triangles 1280, step size 1.4 Å) is 0.221 + 0.131 + 0.982 = 1.334 seconds (on an Iris Indy workstation).

An example of our method of approximation applied to the molecular and the solvent-accessible surface is shown in Figure 9.

TABLE I.
CPU Times (Iris Indy) Used to Calculate Embracing Ellipsoid and to Analytically Determine Pieces of Molecular Surfaces, Where *rp* = 1.5 Å.

Type	Code[a]	Atoms	Triangles	Convex	Toroidal	Concave	CPU[b] (s)	CPU[c] (s)
Ligand	7tmn	33	1280	33	99	70	0.221	0.131
Ligand	9lyz	53	1280	52	158	110	0.238	0.317
DNA	8bna	243	5120	206	636	448	0.616	11.912
Protein	1crn	327	5120	234	708	484	0.626	20.445
RNA	5tra	1822	20,480	1323	4275	3128	2.411	867.055

[a]The entries of the protein in the PDB database.
[b]To calculate the embracing ellipsoid.
[c]To determine analytically the surface pieces.

TABLE II.
The CPU Times (Iris Indy) Used to Deflate Starting Ellipsoid Toward Solvent-Accessible Surface, Where *rp* = 1.5 Å.

	Number of:		SAS (step size = 1.4 Å)			SAS (step size = 10.0 Å)		
Code[a]	Atoms	Triangles	Steps	CPU (s)	ACPU (s)[b]	Steps	CPU (s)	ACPU (s)[b]
7tmn	33	1280	6	0.154	0.026	1	0.096	0.096
9lyz	53	1280	7	0.301	0.043	1	0.114	0.114
8bna	243	5120	18	12.746	0.708	3	2.612	0.871
1crn	327	5120	10	32.876	3.288	2	8.128	4.064
5tra	1822	20,480	30	616.345	20.545	5	104.861	20.972

[a]The entries of the protein in the PDB database.
[b]The average CPU times per step.

COMPARISON OF TRIANGULAR MESH AND QUADRILATERAL MESH METHODS

The proposed method, as implemented in the aforementioned algorithm presents two refinements compared with the quadrilateral mesh method we used initially. This first refinement of our procedure concerns the replacement of the embracing sphere by an embracing ellipsoid. This ellipsoid was obtained from the deformation of the starting embracing sphere according to the three principal axes of the target molecule. The other refinement involves the use of a triangular mesh, which was obtained from an icosahedron subdivision sphere procedure and provides the advantage of a highly uniform vertex distribution, as opposed to a rectangular mesh built from the meridian and parallel representation on a sphere that has a high density of polygons in its polar regions. Table IV provides a comparison of CPU times by using these two methods, when the step size was set to 3.0 Å, and the radius of probe was set to 1.5 Å. For the triangular mesh method and the quadrilateral mesh method, the triangular faces and quadrilateral faces on the surfaces are 5120 and 2870, respectively, and the vertices are 2562 and 2940, respectively.

SURFACE AREA AND VOLUME

As all the faces are triangles and the embraced volume is a polyhedron, the surface area and volume can easily be calculated. For the thermolysin substrate molecule, the method gives a surface area of 392.527 $Å^2$ and a volume of 397.522 $Å^3$ (with 2562 points, 5120 triangles as in Fig. 9a, the probe radius is 1.5 Å). The analytical molecular surface area and volume computed by the Connolly program are 391.751 $Å^2$ and 399.958 $Å^3$ (the probe radius is 1.5 Å). There is a discrepancy between these two methods. The main reason for this discrepancy originates from the regions with re-entrant features. Therefore, the larger the re-entrant surface portion and the more the significant re-entrant shape, the higher the discrepancy.

TABLE III.
CPU Times (Iris Indy) Used to Deflate Starting Ellipsoid Toward the Molecular Surface, Where *rp* = 1.5 Å.

	Number of:		MS (step size = 1.4 Å)		
Code[a]	Atoms	Triangles	Steps	CPU (s)	ACPU (s)[b]
7tmn	33	1280	6	0.982	0.1964
9lyz	53	1280	7	1.775	0.2536
8bna	243	5120	18	11.912	0.7445
1crn	327	5120	10	48.375	4.0312
5tra	1822	20,480	30	3276.171	93.605

[a]The entries of the protein in the PDB database.
[b]The average CPU times per step.

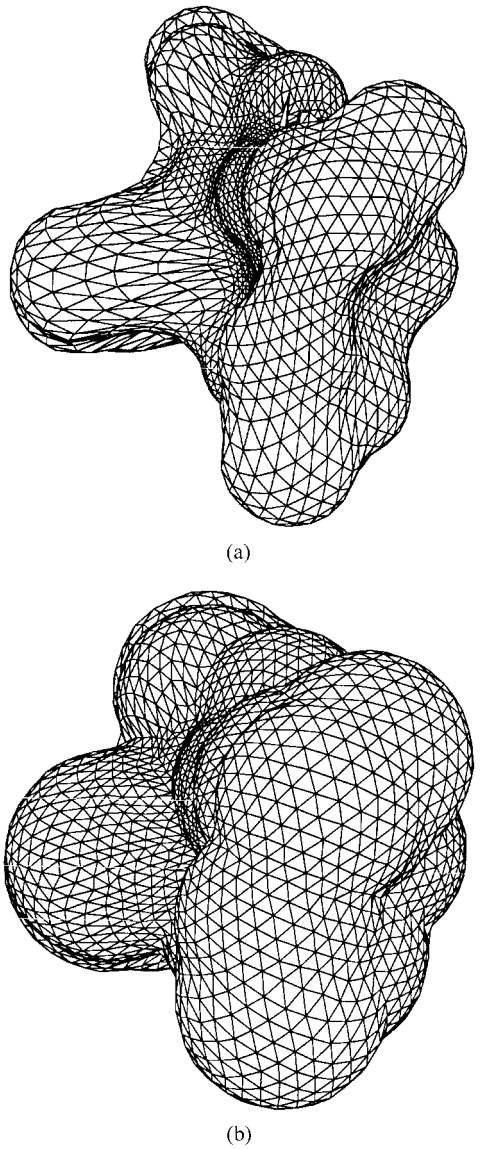

FIGURE 9. An example of approximation to the surface of the thermolysin substrate molecule (7tmn, 33 atoms) with hidden-line removal, obtained from the triangular mesh on the embracing ellipsoid with 2562 vertices and 5120 triangles: (a) to the molecular surface (radius of probe = 1.5 Å, step size = 0.5 Å); and (b) to the solvent-accessible surface (radius of probe = 1.5 Å, step size = 0.5 Å).

TABLE IV.
Comparison of Triangular and Quadrilateral Methods.[a]

	Triangular mesh			Quadrilateral mesh		
Atoms	Triface	Steps	CPU (s)	Quadri-face	Steps	CPU (s)
26	5120	2	0.238	2870	2	0.368
53	5120	3	0.661	2870	3	0.909
327	5120	5	4.178	2870	5	5.171
473	5120	6	7.741	2870	7	12.014

[a]Considers the CPU times (on Iris Indy) used to obtain the solvent-accessible surfaces, where *rp* = 1.5 Å and Step size = 3.0 Å.

Conclusions

The method presented herein considers analyses of all elements of the molecular surface, calculation of the embracing ellipsoid of the protein molecule, and an iterative deflation procedure to obtain the final envelope molecular surface. The elements of the molecular surface were classified as convex pieces, concave pieces (spherical triangles), and tori, contiguous with each other. A triangular mesh that was well-distributed and connected by grid points was built on the embracing ellipsoid calculated from the coordinates of the atoms of the molecule. A final grid surface was then obtained by iteratively deflating all grid points to the best point on the molecular surface. The deflating direction affected the surface obtained. Depending on the probe radius and atom radii, the van der Waals surface, molecular surface, and solvent-accessible surface can be obtained using this method.

It was shown in the present study that this method of mapping the triangular mesh on the starting embracing ellipsoid is a very useful tool for obtaining a molecular embracing surface. As it is a one-to-one mapping, a unique spherical coordinate (θ, φ) can be assigned to each point on the surface, and spherical harmonic expansion coefficients can be computed directly from the Cartesian coordinates of these points and the spherical coordinates.[35]

For the doughnut-like surface, some grid points will cross the embracing ellipsoid during the deflation procedure. As these points are not convergent, we cannot get an embracing surface. Therefore, our method is not suitable for such surfaces as this case cannot be checked beforehand in our program.

Acknowledgments

The authors thank the Université Henri Poincaré Nancy I and the University of Science and Tech-

nology, China, for everything that they have done in this collaboration.

References

1. C. Chothia, *Nature*, **248**, 338 (1974).
2. C. Chothia, *Nature*, **254**, 304 (1975).
3. D. Eisenberg and A. D. Mclachlan, *Nature*, **319**, 199 (1986).
4. L. Wesson and D. Eisenberg, *Prot. Sci.*, **1**, 227 (1992).
5. C. A. Schiffer, J. W. Caldwell, R. M. Stroud, and P. A. Kollman, *Prot. Sci.*, **1**, 396 (1992).
6. C. A. Schiffer, J. W. Caldwell, P. A. Kollman, and R. M. Stroud, *Molec. Simul.*, **10**, 121 (1993).
7. B. V. Freyberg and W. Braun, *J. Comput. Chem.*, **14**, 121 (1993).
8. B. V. Freyberg, T. J. Richmond, and W. Braun, *J. Mol. Biol.*, **233**, 275 (1993).
9. T. Ooi, M. Ootobake, G. Nemethy, and H. A. Scheraga, *Proc. Natl. Acad. Sci.*, **84**, 3086 (1993).
10. K. C. Smith and B. Honig, *Proteins*, **18**, 119 (1994).
11. G. Perrot, B. Cheng, K. D. Gibson, J. Vila, K. A. Palmer, A. Nayeem, B. Maigret, and H. A. Scheraga, *J. Comput. Chem.*, **13**, 1 (1992).
12. J. Cherfils and J. Janin, *Curr. Opin. Struct. Biol.*, **3**, 265 (1993).
13. C. Chothia, *J. Mol. Biol.*, **105**, 1 (1976).
14. J. Miller, J. Janin, A. M. Lesk, and C. Chothia, *J. Mol. Biol.*, **196**, 641 (1987).
15. P. K. Weiner, R. Langridge, J. M. Blaney, R. Schaffer, and P. A. Kollman, *Proc. Natl. Acad. Sci. USA*, **79**, 3754 (1979).
16. M. L. Connolly, *Science*, **221**, 709 (1983).
17. A. J. Morffew, *Adv. Biotechnol. Proc.*, **5**, 31 (1985).
18. D. Avnir, D. Farin, and P. Pfeifer, *Nature*, **308**, 261 (1984).
19. T. E. Klein, C. C. Huang, E. F. Pettersen, G. S. Couch, T. E. Ferrin, and R. Langridge, *J. Mol. Graphics*, **8**, 16 (1990).
20. C. Katchalski-Katzir, I. Shariv, M. Eisenstein, A. A. Friesem, C. Aflalo, and I. Vakser, *Proc. Natl. Acad. Sci. USA*, **89**, 2195 (1992).
21. A. N. Jain, T. G. Dietterich, R. H. Lathrop, D. Champman, R. E. Critchlow Jr., B. E. Bauer, T. A. Webster, and T. Lozano-Perez, *J. Comput.-Aided Mol. Des.*, **8**, 635 (1994).
22. P. D. J. Grootenhuis, D. C. Roe, P. A. Kollman, and I. D. Kuntz, *J. Comput.-Aided Mol. Des.*, **8**, 731 (1994).
23. R. Norel, S. L. Lin, H. J. Wolfson, and R. Nussinov, *Biopolymers*, **34**, 933 (1994).
24. R. L. DesJarlais and J. S. Dixon, *J. Comput.-Aided Mol. Des.*, **8**, 231 (1994).
25. B. K. Shoichet and I. D. Kuntz, *Prot. Eng.*, **6**, 723 (1993).
26. M. C. Lawrence and P. M. Colman, *J. Mol. Biol.*, **234**, 946 (1993).
27. B. K. Shoichet and I. D. Kuntz, *J. Mol. Biol.*, **221**, 327 (1991).
28. R. J. Zauhar and R. S. Morgan, *J. Comput. Chem.*, **11**, 603 (1990).
29. B. J. Yoon and A. M. Lenhoff, *J. Comput. Chem.*, **11**, 1080 (1990).
30. A. H. Juffer, E. F. F. Botta, B. A. M. van Keulen, A. van der Ploeg, and H. J. C. Berendsen, *J. Comput. Phys.*, **97**, 144 (1991).
31. Z. Xiang, Y. Shi, and Y. Xu, *J. Comput. Chem.*, **16**, 512 (1995).
32. M. Zehfus and G. D. Rose, *Biochemistry*, **25**, 5759 (1986).
33. M. Zehfus, *Proteins*, **16**, 293 (1993).
34. B. S. Duncan and A. J. Olson, *J. Mol. Graphics*, **13**, 250 (1995).
35. B. S. Duncan and A. J. Olson, *Biopolymers*, **33**, 219 (1993).
36. M. L. Connolly, *J. Appl. Cryst.*, **16**, 548 (1983).
37. M. L. Connolly, *J. Appl. Cryst.*, **18**, 499 (1985).
38. B. Lee and F. M. Richards, *J. Mol. Biol.*, **55**, 379 (1971).
39. F. M. Richards, *Ann. Rev. Biophys. Bioeng.*, **6**, 151 (1977).
40. M. F. Sanner, A. J. Olson, and J.-C. Spehner, *Biopolymers*, **38**, 305 (1996).
41. A. Dietrich and B. Maigret, *J. Mol. Graphics*, **9**, 85 (1991).